Iraqi journal of Bioscience and Biomedical
Published Online First: 30 / June /2026.
p-ISSN: 3007-5491 / e-ISSN:3007-5505

Green Synthesis of Gold Nanoparticles using Heliotropium europaeum: Crude Extract and Purified Flavonoids

[1]Maryam F.  ***and [2]Oraibi A.G.***

[1,2] Department of Plant Biotechnology, College of Biotechnology, Al-Nahrain University, Baghdad, Iraq.

*Corresponding author: MaryamFouadh217@gmail.com

Received: 2/5/2026, Accepted: 5/6/2026, Published: 30/6/2026.

Abstract

This study aims to green synthesis gold nanoparticles using aqueous extract of *Heliotropium europaeum* (family Boraginaceae) from Sulaymaniyah, Iraq, and characterize their physicochemical properties. A comparative approach was employed using crude extract, AuNPs synthesized from crude extract, and AuNPs synthesized from purified flavonoid. Aqueous extract was prepared from shade-dried plant. AuNPs were synthesized by reacting 100 ml extract with 20 mL of 1 mM $HAuCl_4$ solution (45°C, 3 hours). Characterization employed UV-Vis spectroscopy, FTIR, AFM, and SEM-EDX. FTIR confirmed the presence of hydroxyl, aliphatic, and aromatic groups in the crude extract, while flavonoid-AuNPs showed metal-O bonds, indicating successful nanoparticle capping. UV-Vis revealed phenolic absorption at 278 nm in the crude extract and characteristic flavonoid bands (520 and 550 nm) in the flavonoid-AuNP sample, confirming their role in bioreduction. SEM showed only large aggregates without nanoparticles for the crude extract, whereas flavonoid-AuNPs displayed aggregated structures of smaller nanoparticles with elemental gold confirmed by EDX. AFM demonstrated that purified flavonoids yielded gold nanoparticles with mean diameters as low as 74.45 nm and a predominance of sub-100 nm particles, unlike the nanoparticles from the crude extract, which formed larger structures with mean diameters of 119.4 nm. The crude extract achieved the larger diameter of 136.3 nm. The results indicate that purified flavonoids from *Heliotropium europaeum* are effective reducing and capping agents, producing smaller and more uniform AuNPs compared to the crude extract.

Keywords: Green Synthesis, Gold nanoparticles (AuNPs), *Heliotropium europaeum*, FTIR, AFM, SEM-EDX, UV-Vis.

Introduction

The genus *Heliotropium* (Boraginaceae) comprises approximately 250-300 species with a global distribution [1]. Various species have a long history of use in traditional medicine for treating fever, gout, and rheumatism, as well as for their anti-inflammatory, antiseptic, and wound-healing properties [2]. This therapeutic potential is attributed to a rich profile of secondary metabolites, including pyrrolizidine alkaloids (PAs), phenolic compounds, terpenoids, and quinones [3,4]. Among these, PAs are the most

Iraqi journal of Bioscience and Biomedical
Published Online First: 30 / June /2026.
p-ISSN: 3007-5491 / e-ISSN:3007-5505

characteristic bioactive constituents, exhibiting anti-tumoural, anti-viral, and anti-microbial activities; however, they are also well known for their hepatotoxicity, which has limited their clinical application despite past evaluations in human cancer trials [2,5].

Approximately 6,000 plant species manufacture PAs, making them one of the most common groups of hepatotoxic plants affecting both humans and animals [6]. In *Heliotropium europaeum,* the concentration and composition of PAs are genetically determined and vary according to the plant organ, developmental stage, and environmental factors such as soil nutrients, climate, and herbivore pressure [5]. Besides alkaloids, flavonoids and other phenolic are abundantly present in the genus and contribute to its antimicrobial and ecological properties [7].

In recent years, nanotechnology has emerged as a promising strategy to enhance the therapeutic index of bioactive natural products while mitigating their toxicity. Gold nanoparticles (AuNPs), in particular, have attracted considerable interest because of their special size-dependent physicochemical properties, including surface plasmon resonance (SPR), high stability, biocompatibility, and ease of surface functionalization [8]. These features permit AuNPs to serve as multifunctional platforms for drug delivery, biosensing [9], and targeted therapy, with dimensions comparable to those of proteins, DNA, and other critical biomolecules [10].

The green synthesis of nanoparticles using plant extracts provides additional advantages over conventional physical or chemical approaches [11], as it avoids toxic reagents and yields nanoparticles that are often more biocompatible and biologically active due to the capping effect of phytochemicals [12]. Plant-mediated synthesis also enables controlled releasing, targeted delivery, and enhanced therapeutic outcomes [13]. In this context, using extracts or purified bioactive fractions from *Heliotropium europaeum* for the green synthesis of AuNPs represents a promising approach that utilizes the phytochemical diversity of the genus as effective reducing and stabilizing agents without the need for toxic chemical reagents [12,13].

However, the synthesis of gold nanoparticles using purified flavonoids from *Heliotropium europaeum* via a green approach has not yet been systematically reported. Therefore, this study aims to synthesize gold nanoparticles using purified flavonoids extracted from *Heliotropium europaeum* through a green synthesis method and to characterize the resulting nanoparticles in terms of their physicochemical properties, including size, morphology, surface charge, and colloidal stability. In addition, a comparative analysis with the crude extract is performed to evaluate the advantages of using a purified bioactive fraction.

Materials and Methods

Study design and sample collection:

The parts of *Heliotropium europaeum* were collected in August 2025 locally from several areas in Sulaymaniyah, Iraq, taking into account environmental conditions such as avoiding plants treated with pesticides. According to the morphological description, the plant was scientifically identified as *Heliotropium europaeum* at the College of Agriculture/Al-Qadisiyah University.

Preparation of the aqueous extract:

Iraqi journal of Bioscience and Biomedical
Published Online First: 30 / June /2026.
p-ISSN: 3007-5491 / e-ISSN:3007-5505

The aqueous plant extract of *Heliotropium europaeum* was prepared as follow [14]: by thoroughly washing the plant parts with water to remove contaminants from the surface, followed by three days of air drying. Fifty grams of plant were ground and put in a 500 mL glass beaker with a capacity containing 250 mL of sterilized distilled water. The mixture was then shaken at 45°C for 24 hours, and the extract was filtered with filter paper and stored at 4°C for future use.

Preparation of gold chloride ($HAuCl_4$) solution

A concentration (1mM) of gold chloride solution was prepared using the following equation:

$$M(M) = \frac{W(g)}{M.wt(g/mol)} \times \frac{1000}{V(mL)}$$

A 1 mM solution of gold(III) chloride trihydrate ($HAuCl_4 \cdot 3H_2O$) was prepared by dissolving 0.0232 g in 100 mL of deionized water.

Partial purification of total flavonoids

The aqueous extract of *Heliotropium europaeum* was concentrated and dissolved in 15 mL of methanol. The solution was then added to a silica gel column (2.5 × 40 cm). Ethyl acetate: methanol (5:5, 100 mL) was used to elute the column. The eluate was collected in vials and observed, then dried with a rotary evaporator. Aluminum chloride ($AlCl_3$) was used in a qualitative flavonoid test to verify the presence of flavonoids in the sample.

Drying procedure:

The aqueous extract and purified flavonoid were put in glass petri dishes and placed in an oven at 45°C for 7-9 days for drying. The resulting powder was collected and stored away from light, air, and moisture for future use.

Biosynthesis of gold nanoparticles Au NPs:

Biosynthesis was carried out using both the aqueous extract and the purified flavonoid.

Using the aqueous extract:

100 mL of the aqueous extract of *Heliotropium europaeum* was mixed with 20 mL of the 1 mM gold chloride solution, and the mixture was heated on a magnetic stirrer plate (45°C, 3 h and pH range 6.0-7.5). The color of the mixture was changed and observed as preliminary evidence of the formation of gold nanoparticles.

Using the purified flavonoid:

A solution of the purified flavonoid powder (10 mg/mL) was prepared in distilled water. Then, 100 mL of this solution was mixed with 20 mL of the 1 mM gold chloride solution and heated on a magnetic stirrer plate at 45°C for 3 h and pH range (5.0-6.5). The color change was similarly monitored as an indicator of nanoparticle formation.

Iraqi journal of Bioscience and Biomedical
Published Online First: 30 / June /2026.
p-ISSN: 3007-5491 / e-ISSN:3007-5505

Additionally, 100 mL of the 1 mM gold chloride solution was kept as a control for some measurements.

Fourier Transform Infrared Spectroscopy

FTIR spectra were recorded using a spectrometer in the range of 4000–400 cm^{-1} with a resolution of 4 cm^{-1}. Samples were measured as KBr pellets.

Ultraviolet-visible spectrometer:

UV-Vis absorption spectra were recorded using a spectrophotometer in the range of 200–1000 nm with a 1 nm resolution.

Scanning Electron Microscopy (SEM):

SEM images and energy-dispersive X-ray (EDX) analysis were performed using a SEM operated at an accelerating voltage of 15 kV. Samples were deposited on carbon tape and sputter-coated with gold.

Atomic Force Microscope (AFM):

AFM images were obtained using a AFM in non-contact mode. Samples were prepared by drop-casting onto freshly cleaved mica and dried at room temperature. Particle size analysis was performed at least 100 particles per sample.

Results and Discussion

Characterization of *Heliotropium europaeum* green synthesis gold nanoparticles:

Characterization was carried out using Fourier Transform Infrared Spectroscopy (FTIR), Ultraviolet-Visible Spectroscopy (UV-Vis), Scanning Electron Microscopy (SEM), and Atomic Force Microscopy (AFM). All examinations were conducted at the Phi Nano-Science Center, Baghdad, Iraq.

Fourier Transform Infrared Spectroscopy (FTIR)

The functional groups involved in the reduction and stabilization of gold nanoparticles[15,16] were identified with an FTIR analysis. Three samples were analyzed: crude extract, AuNPs synthesized from the crude extract, and AuNPs synthesized from flavonoids.

Iraqi journal of Bioscience and Biomedical
Published Online First: 30 / June /2026.
p-ISSN: 3007-5491 / e-ISSN:3007-5505

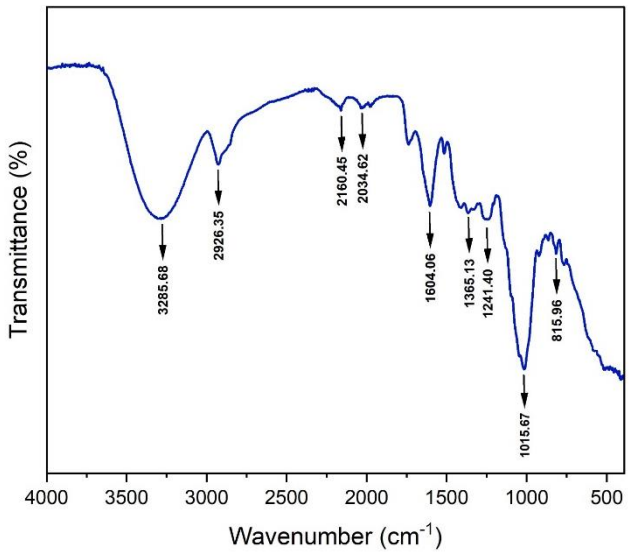

Figure 1: The FTIR spectrum of the crude extract.

The result of FTIR analysis of crude extract showed (Fig. 1) that in its spectrum broad O–H stretch (3285 cm^{-1}) [17], C–H stretch (2926 cm^{-1}) [18,19], and C=O stretch (1604 cm^{-1}) [17,20].

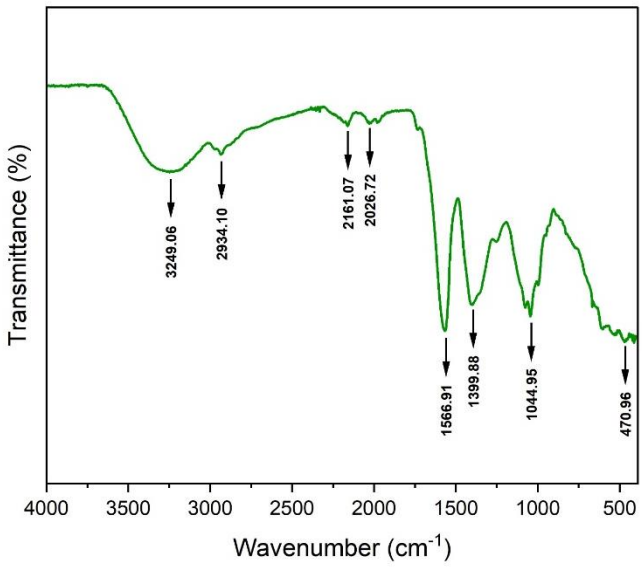

Figure 2: The FTIR spectrum of AuNPs synthesized by crude extract.

The result of FTIR analysis of the AuNPs synthesized by crude extract showed that it (Fig. ٢) exhibited characteristic bands at 3219 cm^{-1} (O–H stretching of hydroxyl groups) [21,22], 2925 cm^{-1} (C–H stretching of aliphatic groups) [23,24], 1560 cm^{-1} (aromatic C=C stretching) [25], 1407 cm^{-1} (C–H bending and O–H bending) [25,26], and 1046 cm^{-1} (C–O stretching)[27]. These bands were existence the flavonoids, phenolic compounds, and polysaccharides, which supported Singh, R. & Mendhulkar's findings [٢٨]. Distinct Au–O

Iraqi journal of Bioscience and Biomedical
Published Online First: 30 / June /2026.
p-ISSN: 3007-5491 / e-ISSN:3007-5505

bands were also observed at approximately 4١١ cm^{-1} and 4٧٠ cm^{-1} [29], confirming effective capping by bioactive reducing compounds. This result is in agreement with Pal, Rajat, *et al.* that report the interaction of gold nanoparticles with bioflavonoids [30].

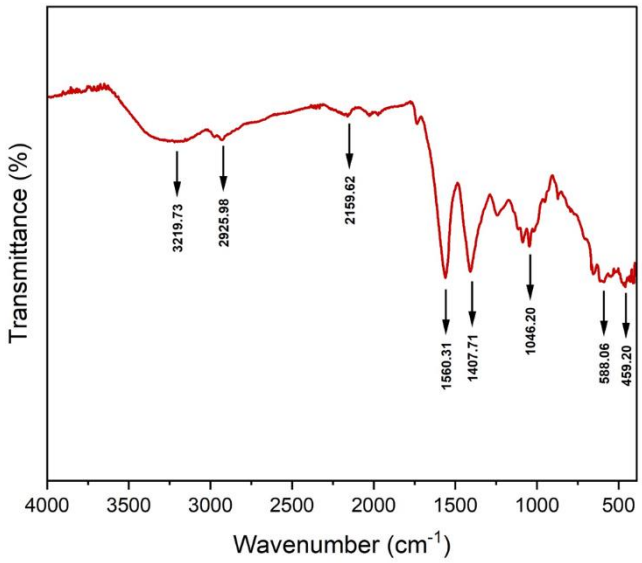

Figure 3: The FTIR spectrum of AuNPs synthesized by purified flavonoid.

The result of FTIR analysis of AuNPs synthesized by purified flavonoid showed that it (Fig. 3) exhibited characteristic bands at 3219 cm^{-1} (O–H stretching of hydroxyl groups) [21], 2925 cm^{-1} (C–H stretching of aliphatic groups) [23,24], 1560 cm^{-1} (aromatic C=C stretching) [25], 1407 cm^{-1} (C–H bending and O–H bending) [25,26], and 1046 cm^{-1} (C–O stretching)[27]. These bands indicate the existence of flavonoids, phenolic compounds, and polysaccharides, that supported by Singh, R. & Mendhulkar's findings [٢٨]. In addition observed two low-wavenumber peaks appeared at 538 cm^{-1} and 459 cm^{-1}, corresponding to metal–oxygen (Au–O) vibrations [16]. This indicates successful binding of the phytochemicals to the gold nanoparticle surface. These findings agree with those reported by Song, J. Y., and Kim, B. S. pertaining to five plant leaf extracts (Pine, Persimmon, Ginkgo, Magnolia, and Platanus) using silver nanoparticles [31].

These FTIR results collectively demonstrate that both the crude extract and the purified flavonoid fraction contain functional groups capable of reducing gold ions and stabilizing the nanoparticles. The presence of Au–O vibrations in both nanoparticle samples indicates chemisorption of the phytochemicals onto the gold surface, which is essential for preventing aggregation and maintaining stability.

Ultraviolet-visible spectrometer (UV-Vis)

The result of UV-Vis analysis of crude extract showed an absorption band in the UV region ٢٥٠-٣٠٠ nm, characteristic of phenolic compounds [32]. The absence of absorption in visible region suggests a lack of extended conjugation among the phytochemical constituents. In contrast, the result of AuNPs synthesized by crude extract showed in (Fig. ٤-b) exhibited a peak at ٥٠٠-٥٥٠ nm range, which falls within Band II (240–295 nm) typical of the benzoyl system in flavonoids [33,34].

Iraqi journal of Bioscience and Biomedical
Published Online First: 30 / June /2026.
p-ISSN: 3007-5491 / e-ISSN:3007-5505

The result of UV-Vis analysis of AuNPs synthesized by purified flavonoid sample showed in (Fig. 4-c) displayed peaks at 520-550 nm range. These results confirm that flavonoids are primarily responsible for the bio-reduction of gold ions [33,34].

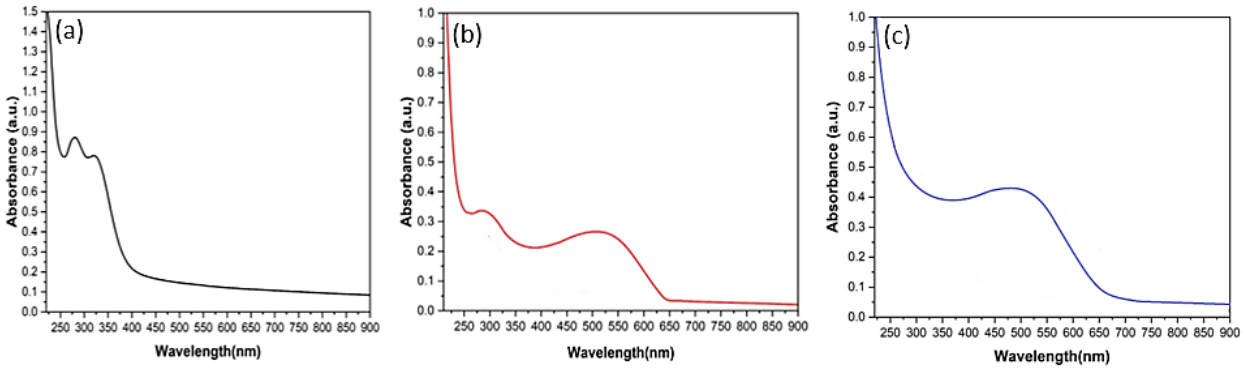

Figure 4: The UV–Vis absorption spectra (200–900 nm) of: (a) crude extract, (b) AuNPs synthesized by crude extract, and (c) AuNPs synthesized by purified flavonoid.

UV-Vis spectroscopy revealed that the crude extract contained phenolic compounds absorbing in the UV-Vis 275 nm and 325 nm with no absorption in the visible region, indicating the absence of extended conjugation systems. This agrees with what researchers Guemari, F. *et al.* have stated in their studies, where they showed that UV-Vis spectroscopy spectra of plant extracts usually appear within the range (200–500 nm), which reflects the presence of phenolic compounds and bioactive substances [35]. After the synthesis of gold nanoparticles (AuNPs) using the crude extract, a characteristic absorption peak appeared at 500 nm, which is the surface plasmonic (SPR) peak of the gold nanoparticles. The presence of flavonoids was confirmed by the II band (280 nm). This aligns with what Indra Ojha, Prem Singh Saud *et al.* reported regarding the production of silver particles from *Alcea rosea* leaf aqueous extract, with absorption occurring in the ultraviolet and visible spectrum between 300 and 600 nanometers. When using purified flavonoids, the peaks appeared at 520 nm. This is consistent with the results of Jain, P. & Arun, P., which concerned nano films composed of tin sulfide (SnS) and silver, fabricated by thermal evaporation, and which showed two prominent peaks in the 500 nm and 580 nm regions [36]. These results conclusively confirm that flavonoids are primarily responsible for the bio-reduction of gold ions and the formation of gold nanoparticles, and that they play a crucial role in the stabilization of these particles.

Iraqi journal of Bioscience and Biomedical
Published Online First: 30 / June /2026.
p-ISSN: 3007-5491 / e-ISSN:3007-5505

Scanning Electron Microscopy (SEM)

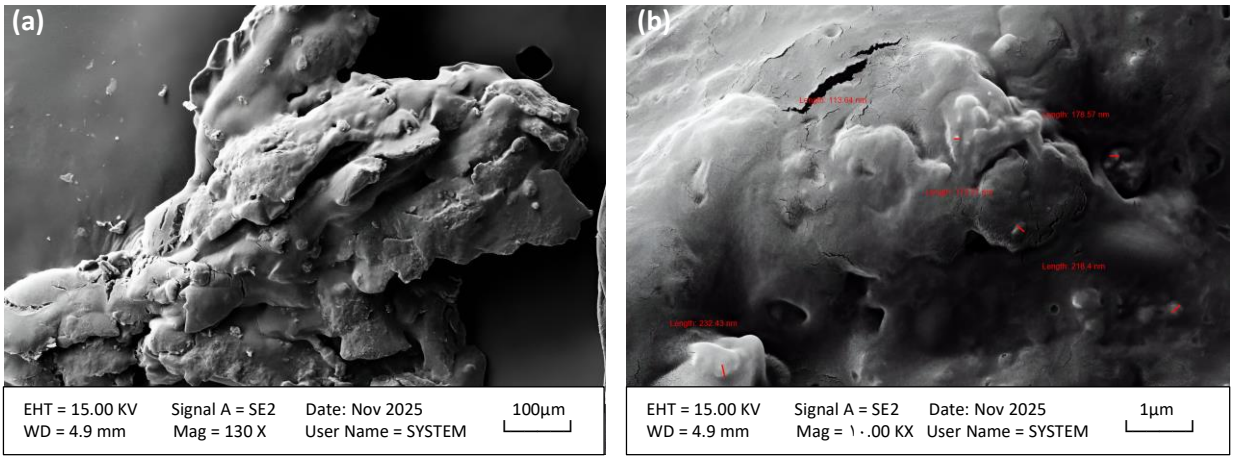

Figure 5: Scanning electron microscopy (SEM) of the crude extract with AuNPs: (a) 130× magnification (b) ١0.00× magnification.

Scanning Electron Microscopy (SEM) results of the dried aqueous extract of *Heliotropium europaeum* (Fig. 5) revealed an irregular surface structure consisting of flakes with submicron dimensions with sharp edges, accompanied by fine cracks and fissures resulting from the drying process. The dimensions of these flakes ranged between 114 and 232 nm, which aligns with the findings of Yang *et al.*[37], who demonstrated that the drying step can have a significant impact on the state of agglomeration. The absence of discrete nanoparticles was expected and confirms that any nanoscale formations observed in other samples are the result of the extract's interaction with gold ions, rather than being of plant origin. Furthermore, the flaky structure suggests that the crude extract adopts a porous morphology with a relatively high specific surface area, a characteristic feature of dried plant extracts.

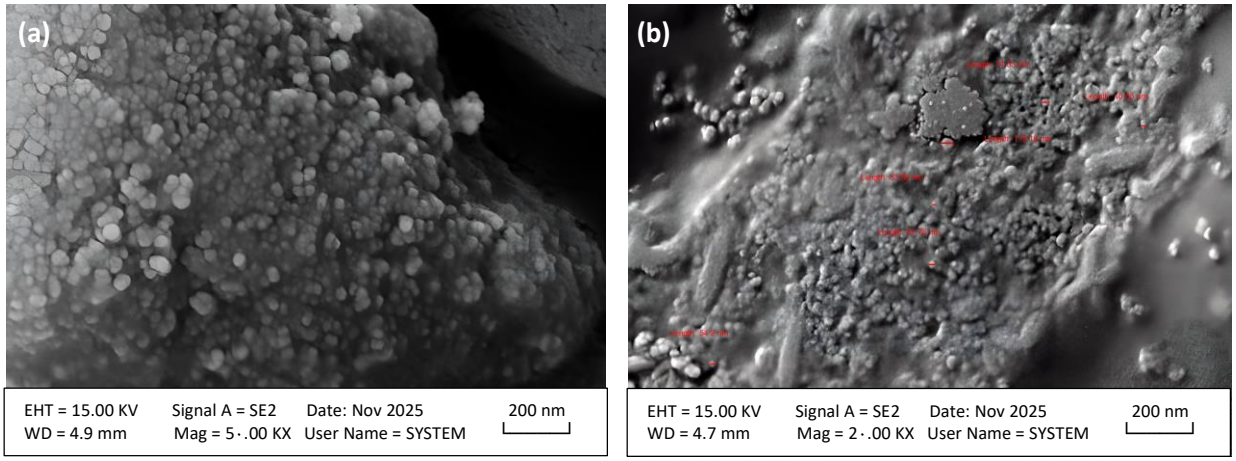

Figure 6: Scanning electron microscopy (SEM) of AuNPs synthesized by crude extract: (a) 50.00× magnification (b) 20.00× magnification.

Iraqi journal of Bioscience and Biomedical
Published Online First: 30 / June /2026.
p-ISSN: 3007-5491 / e-ISSN:3007-5505

The SEM results of the AuNPs synthesized by crude extract (Fig. 6) showed the presence of irregularly shaped aggregates with sizes ranging from 33.88 to 115.18 nm. At high magnification (50.00×), these aggregates were observed to consist of small, densely packed nanoparticles. This demonstrates the ability of the crude extract to reduce gold ions (Au^{3+}) to metallic gold (Au^{0}) and form nanoparticles a finding [38], further confirmed by EDX analysis. The presence of these large-scale structures is attributed to the failure of the crude extract to effectively stabilize the nanoparticles and prevent their aggregation; this failure, in turn, stems from the presence of large molecules (such as proteins and polysaccharides) within the crude extract. This observation aligns with the findings of Talib *et al.*, whose research on the stabilization of gold nanoparticles (GNPs) utilizing a natural plant extract derived from *Aloe vera* indicated that insufficient stabilization inevitably leads to aggregation [39].

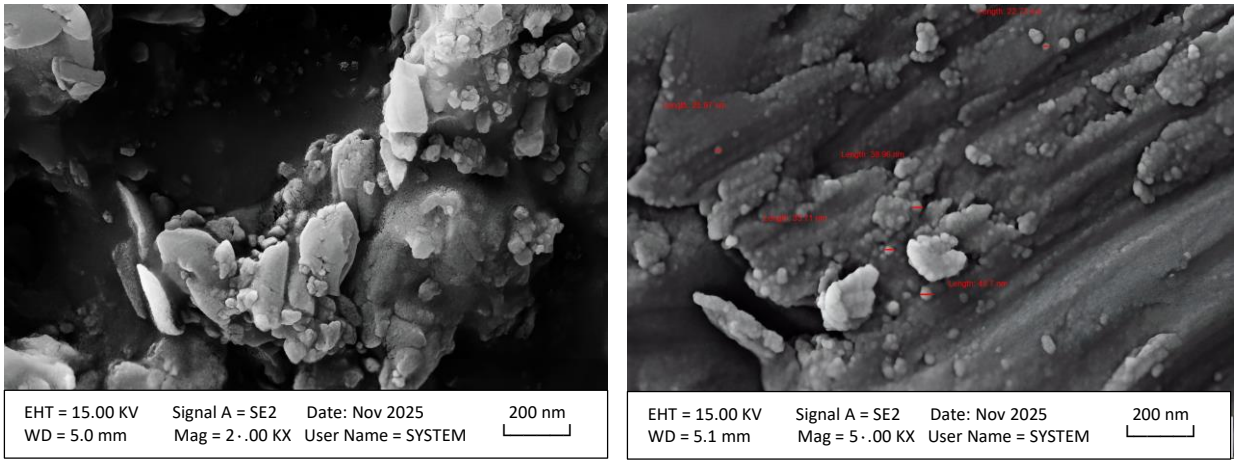

Figure 7: Scanning electron microscopy (SEM) of AuNPs synthesized by purified flavonoid: (a) 20.00× magnification (b) 50.00× magnification.

The SEM results for gold nanoparticles synthesized using purified flavonoid molecules (Fig. 7) demonstrated a notable improvement in morphology and size compared to those synthesized using the crude extract. At a magnification of 50.00×, spherical[40,41] to semi-spherical nanoparticles with nanoscale dimensions were observed, with the diameters of most particles ranging between 22 and 48 nm. While some small aggregates, likely secondary clusters are visible, they are less dense and smaller in size than those observed with the crude extract. Individual particles can be clearly distinguished in several regions of the image, distributed irregularly across the surface of the organic substrate. These result is confirming that purified flavonoids constitute the primary active component responsible for reducing gold ions and stabilizing the resulting nanoparticles. The interfering macromolecules' (such as proteins and polysaccharides) removal led to greater control over the crude synthesis process, leading to more uniform nanoparticles and the formation of smaller ones. Any residual aggregation may be attributed to the concentration of flavonoids or specific reaction conditions. These findings align with what was reported by Lafta *et al.*[42], who utilized *Arctium lappa* a medicinal plant rich in flavonoids for the green synthesis of gold nanoparticles (AuNPs) and silver nanoparticles (AgNPs) to evaluate their antioxidant properties. In that study, the resulting gold nanoparticles ranged in size from 80 to 160 nm, while the silver nanoparticles

Iraqi journal of Bioscience and Biomedical
Published Online First: 30 / June /2026.
p-ISSN: 3007-5491 / e-ISSN:3007-5505

ranged from 20 to 40 nm. This result is also similar to what was achieved by Das *et al.* who obtained gold nanoparticles ranging in size from 20 to 45 nanometers using an aglycone flavonoid, quercetin [43].

The purification of flavonoids from the crude extract is essential for producing gold nanoparticles that are smaller, more uniform, and less aggregated. While the crude extract is suitable for reducing gold ions, it lacks sufficient stabilizing capacity. These findings provide a solid foundation for utilizing purified flavonoids in applications requiring stable and uniformly distributed nanoparticles, particularly in the catalytic fields and biomedical.

Atomic Force Microscope (AFM)

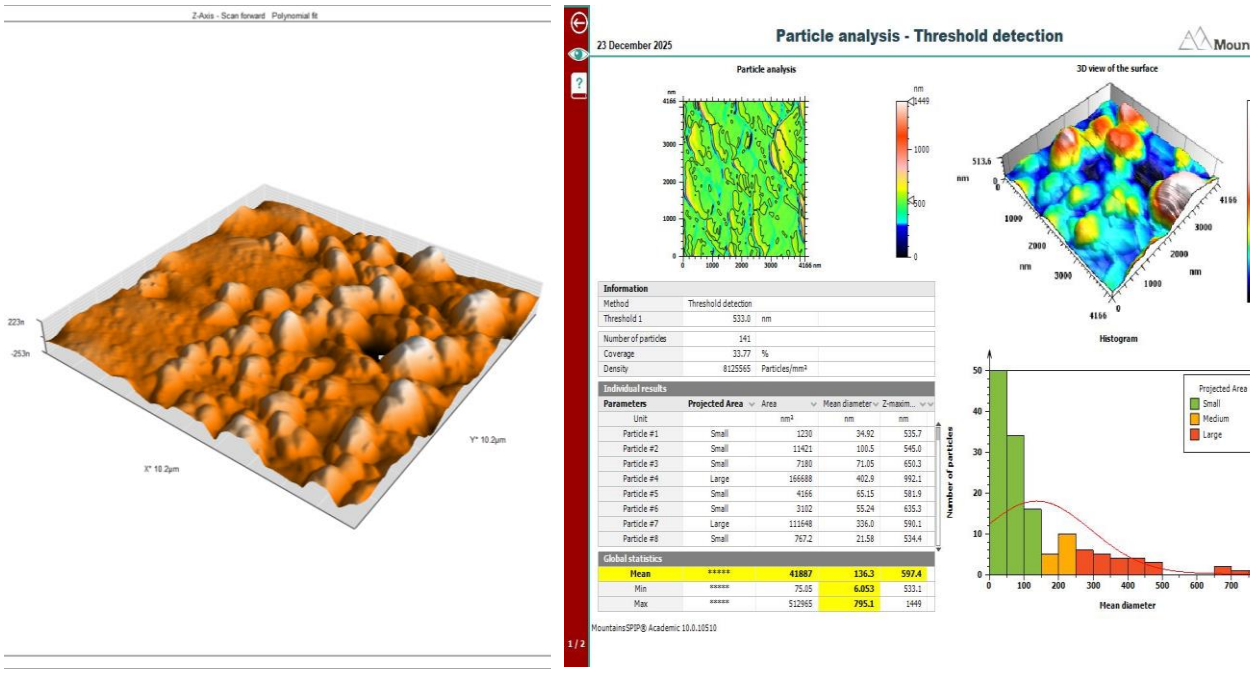

Figure 8: The AFM for crude extract.

The results of AFM crude extract in (Fig. 8) showed the analysis of the raw sample revealed the presence of 141 particles within the scanned area, corresponding to a surface coverage of 34%. Particle diameters (peak diameter) ranged from 21 nm to 402 nm, with an arithmetic mean of 136 nm. Vertical heights (Z-max) ranged from 534 nm to 992 nm (mean: 597 nm). The surface area of the larger particles was approximately 166,688 nm², while smaller particles occupied areas between 767 and 11,421 nm². The particles exhibited irregular shapes and extensive agglomeration.

The AFM analysis of the crude extract showed a significant discrepancy between particle diameters and vertical heights, suggesting that the particles are neither spherical nor flat but rather exhibit an acicular or columnar morphology. Similar behavior has been reported by Williams *et al.* for *Arabidopsis thaliana* seeds rich in the polysaccharide rhamnogalacturonan I (RGI), which tend to form hydrogel networks or vertical aggregates [44]. The low surface coverage, despite the presence of 141 particles, indicates that

Iraqi journal of Bioscience and Biomedical
Published Online First: 30 / June /2026.
p-ISSN: 3007-5491 / e-ISSN:3007-5505

agglomeration reduces packing efficiency, a common feature in raw extracts lacking stabilization. The large variation in particle surface area further confirms the inherent polydispersity of the sample.

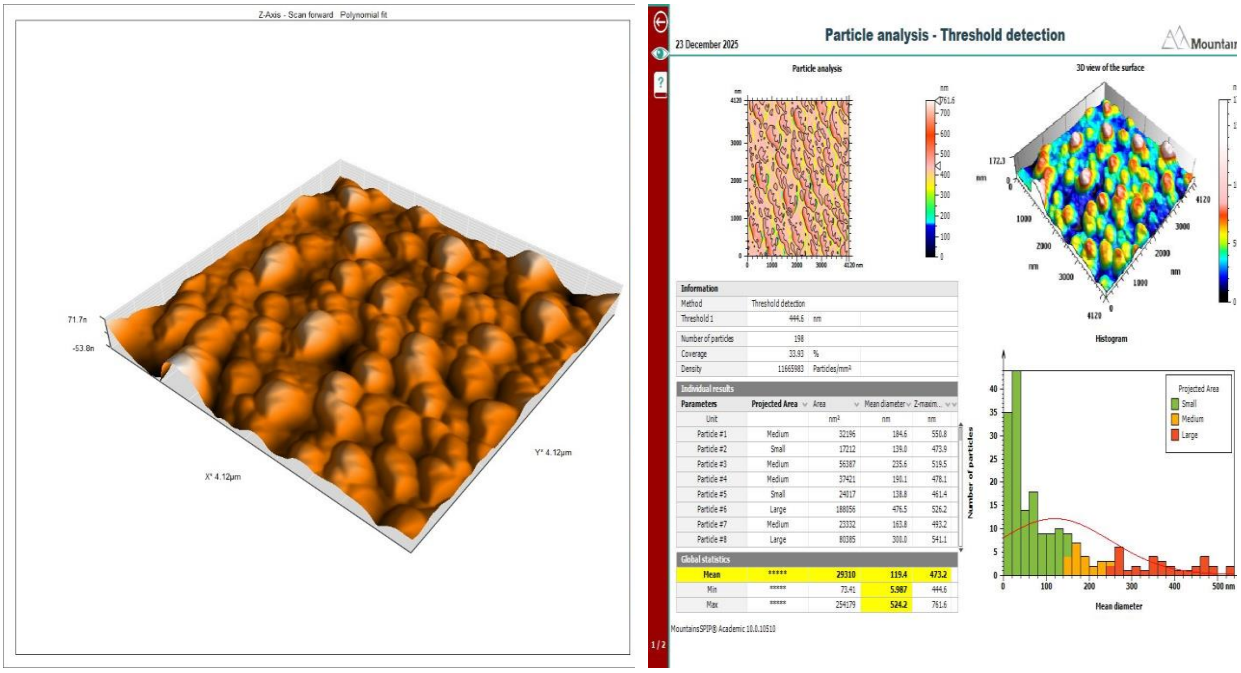

Figure ٩: The AFM of AuNPs synthesized by crude extract.

The result of AFM showed the AuNPs synthesized by crude extract (Fig. 9) showed the presence of 198 particles with a surface coverage of 34%. Particle diameters ranged from 139 nm to 477 nm. Vertical heights (Z-max) ranged between 461 nm and 550 nm. The area of the larger particles was recorded at 188,056 nm², while the area of the smaller particles ranged from 17,212 to 24,017 nm². Compared to the raw sample, a relative enhancement in homogeneity was observed, although some secondary agglomerations remained.

Gold nanoparticles synthesized from the crude extract showed a significant improvement in morphological homogeneity when compared to the crude extract itself, as evidenced by the disappearance of ultrafine particles, a decrease in vertical heights, and a convergence of surface areas. Nonetheless, some secondary agglomeration persisted, indicating that the synthesis conditions should be optimized to produce more uniform particles. These results confirm the capacity of the crude extract to act as both a reducing and stabilizing agent, yet they also highlight the limitations of this crude approach when compared to chemical methods or the use of purified extracts. Elia P *et al.*, found that gold nanoparticles made with *Punica granatum* extract had lower stability and were more likely to agglomerate and form larger particles[45].

Iraqi journal of Bioscience and Biomedical
Published Online First: 30 / June /2026.
p-ISSN: 3007-5491 / e-ISSN:3007-5505

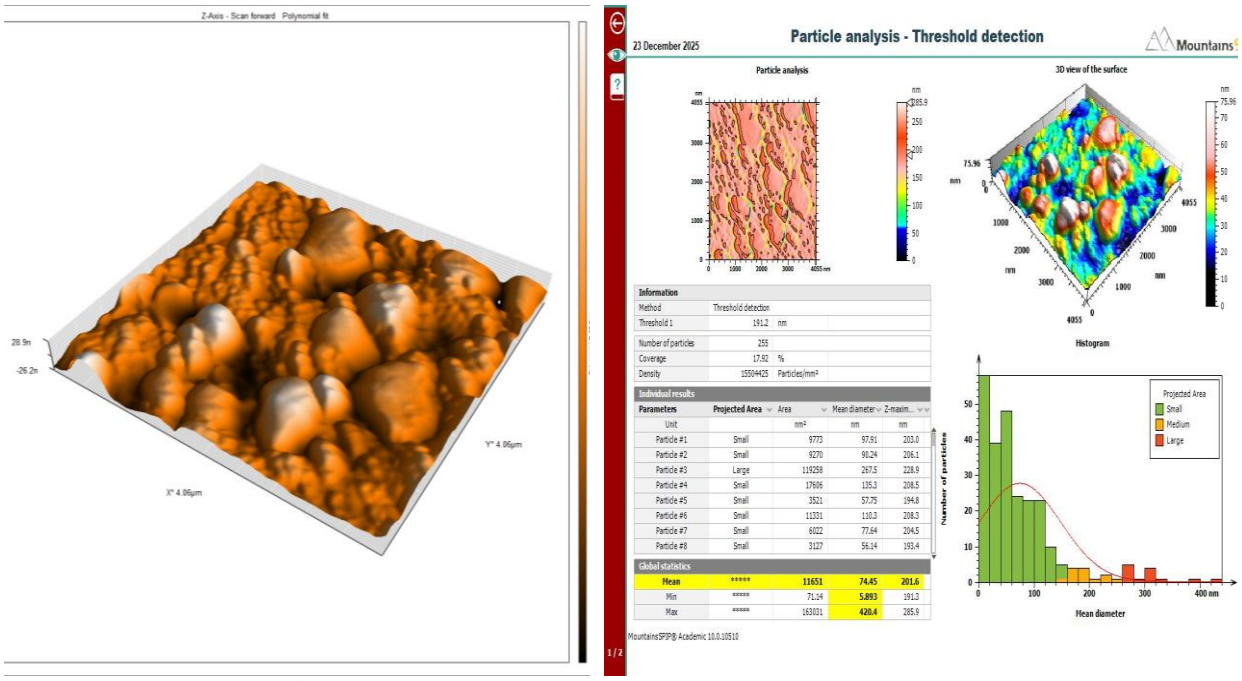

Figure ١٠: The AFM of AuNPs synthesized by purified flavonoid.

The results of AFM analysis of the AuNPs synthesized by the purified flavonoid sample that were shown in (Fig. 10) demonstrated the highest degree of homogeneity among the three samples. A total of 255 particles were detected, with a surface coverage of 18%. Particle diameters ranged from 56 nm to 268 nm, with 75 nm being an average. Vertical heights ranged from 193 nm to 229 nm, values lower than those of the other samples indicating a flatter morphology. The surface area of the larger particles measured 119,258 nm², while that of the smaller particles ranged between 3,127 and 17,606 nm².

Gold nanoparticles synthesized using flavonoids demonstrated a reduction in average diameter compared to the raw sample (decreasing from 136 to 75 nanometers), as well as an increased proportion of particles smaller than 100 nanometers. Also the bulk of the particles observed were sphere-shaped or quasi-sphere-shaped in shape and exhibited minimal aggregation; this confirms the role of flavonoid purification in enhancing stability and reflects an improvement in the efficiency of the reduction processes and stabilization processes. This finding corroborates with work of Dang *et al.*, who utilized flavonoid extracts derived from *Hopea odorata* leaves to serve simultaneously as reducing and stabilizing agents, with results indicating that the size distribution of the gold nanoparticles ranged between 3 and 30 nanometers [46].

Conclusions

In this study, we successfully established an eco-friendly[47,48], cost-effective green synthesis method for gold nanoparticles (AuNPs) using *Heliotropium europaeum* extract obtained from Sulaymaniyah, Iraq. Eliminating the need for toxic chemicals, due to phytochemicals, particularly flavonoids and phenolic compounds, proved highly efficient as both reducing and stabilizing agent. FTIR, UV-Vis, SEM-EDX and AFM analyses were used to comprehensively characterize the formed nanoparticles [49], which were found to be predominantly stable and had a mean diameter of 74.45 nm, a size range suitable for

pharmaceutical[48,50], biomedical and catalytic applications. These findings suggest that the *Heliotropium europaeum* biosynthesized AuNPs could serve as promising candidates for drug delivery systems and pharmaceutical applications. Future potential applications include use *in vitro* and *in vivo* studies required to fully evaluate their therapeutic efficacy, cytotoxicity, and histopathology.

Acknowledgments

I would like to express my deepest gratitude and appreciation to my supervisor for her invaluable guidance and continuous support throughout the practical part of this research. Her direct supervision and hands-on assistance were essential in carrying out the experimental work effectively. Her insightful feedback and scientific advice greatly contributed to overcoming challenges and ensured the successful completion of this study in the best possible manner.

Author's Declaration

- We hereby confirm that all the tables in the paper are original and have been created by us.

References

1. Abdelkhalek, A., Elshaer, M., Abdulaziz, A.-A., Kowalczewski, P., & Behiry, S. (2024). Antimicrobial activities and metabolites profiling of Heliotropium bacciferum Forssk. methanolic extract. *Notulae Botanicae Horti Agrobotanici Cluj-Napoca, 52*(3), 13602-13602.
2. Al-Amin, K., Kawsar, M., Mamun, M., & Sahadat Hossain, M. (2025). Fourier transform infrared spectroscopic technique for analysis of inorganic materials: a review. *Nanoscale Adv, 7*(21), 6677-6702. https://doi.org/10.1039/d5na00522a
3. Al-Amin, K., Kawsar, M., Mamun, M. T. R. B., & Hossain, M. S. (2025). Fourier transform infrared spectroscopic technique for analysis of inorganic materials: a review. *Nanoscale Advances, 7*(21), 6677-6702.
4. Aljabali, A. A. A., Akkam, Y., Al Zoubi, M. S., Al-Batayneh, K. M., Al-Trad, B., Abo Alrob, O., Alkilany, A. M., Benamara, M., & Evans, D. J. (2018). Synthesis of Gold Nanoparticles Using Leaf Extract of Ziziphus zizyphus and their Antimicrobial Activity. *Nanomaterials (Basel), 8*(3). https://doi.org/10.3390/nano8030174
5. Arshad, A., Ahemad, S., Saleem, H., Saleem, M., Zengin, G., Abdallah, H. H., Tousif, M. I., Ahemad, N., & Fawzi Mahomoodally, M. (2021). RP-UHPLC-MS Chemical Profiling, Biological and In Silico Docking Studies to Unravel the Therapeutic Potential of Heliotropium crispum Desf. as a Novel Source of Neuroprotective Bioactive Compounds. *Biomolecules, 11*(1), 53. https://www.mdpi.com/2218-273X/11/1/53
6. Babu, P. J., Sharma, P., Saranya, S., Tamuli, R., & Bora, U. (2013). Green synthesis and characterization of biocompatible gold nanoparticles using Solanum indicum fruits. *Nanomaterials and Nanotechnology, 3*, 4.
7. Boruah, J. S., Devi, C., Hazarika, U., Bhaskar Reddy, P. V., Chowdhury, D., Barthakur, M., & Kalita, P. (2021). Green synthesis of gold nanoparticles using an antiepileptic plant extract: in vitro biological and photo-catalytic activities. *RSC Adv, 11*(45), 28029-28041. https://doi.org/10.1039/d1ra02669k
8. Cojocaru, E., Ghitman, J., Biru, E. I., Pircalabioru, G. G., Vasile, E., & Iovu, H. (2021). Synthesis and characterization of electrospun composite scaffolds based on chitosan-carboxylated graphene oxide with potential biomedical applications. *Materials, 14*(10), 2535.

9. Dang, K.-P. T., Nguyen Ngo, V., Vu_Quang, H., & Nguyen, T.-D. (2025). Gold nanoparticles biosynthesized from flavonoid extract of Hopea odorata leaves and their catalytic activity for 4-nitrophenol reduction. *Journal of Engineering Research, 13*(3), 2517-2526. https://doi.org/https://doi.org/10.1016/j.jer.2024.09.011
10. Das, D. K., Chakraborty, A., Bhattacharjee, S., & Dey, S. (2013). Biosynthesis of stabilised gold nanoparticle using an aglycone flavonoid, quercetin. *Journal of Experimental Nanoscience, 8*(4), 649-655. https://doi.org/10.1080/17458080.2011.591001
11. Dzimitrowicz, A., Cyganowski, P., Jamroz, P., Jermakowicz-Bartkowiak, D., Rzegocka, M., Cwiklinska, A., & Pohl, P. (2019). Tuning Optical and Granulometric Properties of Gold Nanostructures Synthesized with the Aid of Different Types of Honeys for Microwave-Induced Hyperthermia. *Materials, 12*(6), 898. https://www.mdpi.com/1996-1944/12/6/898
12. Elia, P., Zach, R., Hazan, S., Kolusheva, S., Porat, Z., & Zeiri, Y. (2014). Green synthesis of gold nanoparticles using plant extracts as reducing agents. *Int J Nanomedicine, 9*, 4007-4021. https://doi.org/10.2147/ijn.S57343
13. Emam, M., El Raey, M. A., Eisa, W. H., El-Haddad, A. E., Osman, S. M., El-Ansari, M. A., & Rabie, A.-G. M. (2017). Green synthesis of silver nanoparticles from Caesalpinia gilliesii (Hook) leaves: antimicrobial activity and in vitro cytotoxic effect against BJ-1 and MCF-7 cells. *Journal of Applied Pharmaceutical Science, 7*(8), 226-233.
14. Goyal, N., & Sharma, S. K. (2014). Bioactive phytoconstituents and plant extracts from genus Heliotropium. *International Journal of Green Pharmacy (IJGP), 8*(4).
15. Guemari, F., Laouini, S. E., Rebiai, A., Bouafia, A., Meneceur, S., Tliba, A., Majrashi, K. A., Alshareef, S. A., Menaa, F., & Barhoum, A. (2022). UV-Visible Spectroscopic Technique-Data Mining Tool as a Reliable, Fast, and Cost-Effective Method for the Prediction of Total Polyphenol Contents: Validation in a Bunch of Medicinal Plant Extracts. *Applied Sciences, 12*(19), 9430. https://www.mdpi.com/2076-3417/12/19/9430
16. Guo, Q., Guo, Q., Yuan, J., & Zeng, J. (2014). Biosynthesis of gold nanoparticles using a kind of flavonol: Dihydromyricetin. *Colloids and Surfaces A: Physicochemical and Engineering Aspects, 441*, 127-132. https://doi.org/https://doi.org/10.1016/j.colsurfa.2013.08.067
17. J. Jeyakodi Moses, D. a. g., P. Sathish, Description automatically generated, M. Keerthivasan, R.J. Pragadeesh and A. Pranesh (2021). Properties Improvement on Polyester Fabric using Polyvinyl alcohol. *International Journal of Engineering Technologies and Management Research*.
18. Jafarizad, A., Safaee, K., Vahid, B., Khataee, A., & Ekinci, D. (2019). Synthesis and characterization of gold nanoparticles using Hypericum perforatum and Nettle aqueous extracts: A comparison with turkevich method. *Environmental Progress & Sustainable Energy, 38*(2), 508-517.
19. Jain, P., & Arun, P. (2014). Localized surface plasmon resonance in SnS: Ag nano-composite films. *Journal of Applied Physics, 115*(20).
20. Karnwal, A., Jassim, A. Y., Mohammed, A. A., Sharma, V., Al-Tawaha, A. R. M. S., & Sivanesan, I. (2024). Nanotechnology for Healthcare: Plant-Derived Nanoparticles in Disease Treatment and Regenerative Medicine. *Pharmaceuticals, 17*.
21. Kassem, A., Abbas, L., Coutinho, O., Opara, S., Najaf, H., Kasperek, D., Pokhrel, K., Li, X., & Tiquia-Arashiro, S. (2023). Applications of Fourier Transform-Infrared spectroscopy in microbial cell biology and environmental microbiology: advances, challenges, and future perspectives. *Front Microbiol, 14*, 1304081. https://doi.org/10.3389/fmicb.2023.1304081
22. Krishnadev, P., Subramanian, K. S., Lakshmanan, A., Ganapathy, S., Raja, K., & Rajkishore, S. K. (2021). Hydroxypropyl methylcellulose nanocomposites containing nano fibrillated cellulose (NFC) from Agave americana L. for food packaging applications. *BioResources, 16*(4), 8125.
23. Lafta, M. Z., Hameed Al-Samarrai, R. R., & Bouaziz, M. (2025). Green synthesis of silver and gold nanoparticles using quercetin extracted from Arctium lappa by HPLC, Characterization and Estimation

of antioxidant activity. *Results in Chemistry, 13*, 102028. https://doi.org/https://doi.org/10.1016/j.rechem.2025.102028

24. Lin, L. Z., & Harnly, J. M. (2012). Quantitation of flavanols, proanthocyanidins, isoflavones, flavanones, dihydrochalcones, stilbenes, benzoic acid derivatives using ultraviolet absorbance after identification by liquid chromatography-mass spectrometry. *J Agric Food Chem, 60*(23), 5832-5840. https://doi.org/10.1021/jf3006905
25. Mahgoub, S. M., Alawam, A. S., Allam, A. A., Mahmoud, M. R., Elrafey, A., Abdelmohsen, A. H., & Mahmoud, R. (2025). Crystal violet removal from aqueous solution: adsorption studies, Box–Behnken optimization, safety, and reuse in methanol oxidation. *RSC advances, 15*(52), 44373-44391.
26. Mendes, E., Belchior, A., Picollo, F., Alves, M. M., Dinica, R. M., Moura, M. J., Pinheiro, T., & Campello, M. P. C. (2025). Synthesis and characterization of gold-coated nanodiamonds through green chemistry as potential radiosensitizers for proton therapy. *arXiv preprint arXiv:2504.11061*.
27. Milan, J., Niemczyk, K., & Kus-Liśkiewicz, M. (2022). Treasure on the Earth—Gold Nanoparticles and Their Biomedical Applications. *Materials, 15*(9), 3355. https://www.mdpi.com/1996-1944/15/9/3355
28. Milaneze, B. A., Oliveira, J. P., Augusto, I., Keijok, W. J., Côrrea, A. S., Ferreira, D. M., Nunes, O. C., Gonçalves, R. d. C. R., Kitagawa, R. R., Celante, V. G., da Silva, A. R., Pereira, A. C. H., Endringer, D. C., Schuenck, R. P., & Guimarães, M. C. C. (2016). Facile Synthesis of Monodisperse Gold Nanocrystals Using Virola oleifera. *Nanoscale Research Letters, 11*(1), 465. https://doi.org/10.1186/s11671-016-1683-3
29. Mongy, Y., & Shalaby, T. I. (2024). Green synthesis of zinc oxide nanoparticles using Rhus coriaria extract and their anticancer activity against triple-negative breast cancer cells. *Scientific Reports, 14*.
30. Motene, M. V., Maepa, C., & Sigidi, M. T. (2025). Optimizing the Antimicrobial, Antioxidant, and Cytotoxic Properties of Silver Nanoparticles Synthesized from Elephantorrhiza elephantina (Burch.) Extracts: A Comprehensive Study. *Plants, 14*(5), 822. https://www.mdpi.com/2223-7747/14/5/822
31. Noah, N. M., & Ndangili, P. M. (2022). Green synthesis of nanomaterials from sustainable materials for biosensors and drug delivery. *Sensors International, 3*, 100166.
32. Ojha, N., & Das, N. (2017). Optimization and characterization of polyhydroxyalkanoates and its copolymers synthesized by isolated yeasts. *Research Journal of Pharmacy and Technology, 10*(3), 861.
33. Ovalle, J., Ovalle, J., & Garcia, O. (2022). Systematic review of the phytochemical compounds use of Heliotropium indicum taking advantage of its advantage in modern medicine. *J Appl Biotechnol Bioeng, 9*(5), 132-136.
34. Ozntamar-Pouloglou, K.-M., Cheilari, A., Zengin, G., Graikou, K., Ganos, C., Karikas, G.-A., & Chinou, I. (2023). Heliotropium procubens Mill: Taxonomic Significance and Characterization of Phenolic Compounds via UHPLC–HRMS- In Vitro Antioxidant and Enzyme Inhibitory Activities. *Molecules, 28*(3), 1008. https://www.mdpi.com/1420-3049/28/3/1008
35. Pal, R., Panigrahi, S., Bhattacharyya, D., & Chakraborti, A. S. (2013). Characterization of citrate capped gold nanoparticle-quercetin complex: Experimental and quantum chemical approach. *Journal of Molecular Structure, 1046*, 153-163. https://doi.org/https://doi.org/10.1016/j.molstruc.2013.04.043
36. Pasieczna-Patkowska, S., Cichy, M., & Flieger, J. (2025). Application of Fourier Transform Infrared (FTIR) Spectroscopy in Characterization of Green Synthesized Nanoparticles. *Molecules, 30*(3), 684. https://www.mdpi.com/1420-3049/30/3/684
37. Rajakumar, G., Gomathi, T., Abdul Rahuman, A., Thiruvengadam, M., Mydhili, G., Kim, S.-H., Lee, T.-J., & Chung, I.-M. (2016). Biosynthesis and Biomedical Applications of Gold Nanoparticles Using Eclipta prostrata Leaf Extract. *Applied Sciences, 6*(8), 222. https://www.mdpi.com/2076-3417/6/8/222
38. Rasul, M. G. (2018). Conventional extraction methods use in medicinal plants, their advantages and disadvantages. *Int. J. Basic Sci. Appl. Comput, 2*(6), 10-14.

39. Sani, A., Cao, C., & Cui, D. (2021). Toxicity of gold nanoparticles (AuNPs): A review. *Biochemistry and biophysics reports*, *26*, 100991.
40. Singh, R., & Mendhulkar, V. D. (2015). FTIR studies and spectrophotometric analysis of natural antioxidants, polyphenols and flavonoids in Abutilon indicum (Linn) sweet leaf extract. *J. Chem. Pharm. Res*, *7*(6), 205-211.
41. Song, J. Y., & Kim, B. S. (2009). Rapid biological synthesis of silver nanoparticles using plant leaf extracts. *Bioprocess and biosystems engineering*, *32*(1), 79-84.
42. Sysak, S., Czarczynska-Goslinska, B., Szyk, P., Koczorowski, T., Mlynarczyk, D. T., Szczolko, W., Lesyk, R., & Goslinski, T. (2023). Metal Nanoparticle-Flavonoid Connections: Synthesis, Physicochemical and Biological Properties, as Well as Potential Applications in Medicine. *Nanomaterials*, *13*(9), 1531. https://www.mdpi.com/2079-4991/13/9/1531
43. Tábuas, B., Cruz Barros, S., Diogo, C., Cavaleiro, C., & Sanches Silva, A. (2024). Pyrrolizidine alkaloids in foods, herbal drugs, and food supplements: chemistry, metabolism, toxicological significance, analytical methods, occurrence, and challenges for future. *Toxins*, *16*(2), 79.
44. Talib, A., Khan, M. S., Gedda, G., & Hui-Fen, W. (2016). Stabilization of gold nanoparticles using natural plant gel: A greener step towards biological applications. *Journal of Molecular Liquids*, *220*, 463-467. https://doi.org/https://doi.org/10.1016/j.molliq.2016.03.079
45. Taniguchi, M., LaRocca, C. A., Bernat, J. D., & Lindsey, J. S. (2023). Digital Database of Absorption Spectra of Diverse Flavonoids Enables Structural Comparisons and Quantitative Evaluations. *Journal of Natural Products*, *86*(4), 1087-1119. https://doi.org/10.1021/acs.jnatprod.2c00720
46. Tole, T. T., Feso, H. H., & Adane, L. (2024). Phytochemical constituents of the roots of Heliotropium verdcourtii (Boraginaceae). *International Journal of Secondary Metabolite*, *11*(2), 211-219.
47. Tran, U. B., Vo-Tran, N. T., Truong, K. T., Nguyen, D. A., Tran, Q. N., Nguyen, H. Q., Lee, J., & Truong-Lam, H. S. (2025). Synthesis of a multicomponent cellulose-based adsorbent for tetracycline removal from aquaculture water. *Beilstein J Nanotechnol*, *16*, 728-739. https://doi.org/10.3762/bjnano.16.56
48. Williams, M. A. K., Cornuault, V., Irani, A. H., Symonds, V. V., Malmström, J., An, Y., Sims, I. M., Carnachan, S. M., Sallé, C., & North, H. M. (2020). Polysaccharide Structures in the Outer Mucilage of Arabidopsis Seeds Visualized by AFM. *Biomacromolecules*, *21*(4), 1450-1459. https://doi.org/10.1021/acs.biomac.9b01756
49. Wongsa, P., Phatikulrungsun, P., & Prathumthong, S. (2022). FT-IR characteristics, phenolic profiles and inhibitory potential against digestive enzymes of 25 herbal infusions. *Sci Rep*, *12*(1), 6631. https://doi.org/10.1038/s41598-022-10669-z
50. Yang, J., Kornet, R., Ntone, E., Meijers, M. G. J., van den Hoek, I. A. F., Sagis, L. M. C., Venema, P., Meinders, M. B. J., Berton-Carabin, C. C., Nikiforidis, C. V., & Hinderink, E. B. A. (2024). Plant protein aggregates induced by extraction and fractionation processes: Impact on techno-functional properties. *Food Hydrocolloids*, *155*, 110223. https://doi.org/https://doi.org/10.1016/j.foodhyd.2024.110223